Structural Insight into the Inhibition of Human Kynurenine Aminotransferase I/Glutamine Transaminase K[||]

Qian Han,*[,†] Howard Robinson,[‡] Tao Cai,[#] Danilo A. Tagle,[§] and Jianyong Li[†]

Department of Biochemistry, Virginia Tech, Blacksburg, Virginia 24061, Department of Biology, Brookhaven National Laboratory, Upton, New York 11973, OIIB, NIDCR, National Institutes of Health, Bethesda, Maryland 20892-4322, and Neuroscience Center, NINDS, National Institutes of Health, Bethesda, Maryland 2089-29525

Received January 21, 2009

Human kynurenine aminotransferase I (hKAT I) catalyzes the formation of kynurenic acid, a neuroactive compound. Here, we report three high-resolution crystal structures (1.50−1.55 Å) of hKAT I that are in complex with glycerol and each of two inhibitors of hKAT I: indole-3-acetic acid (IAC) and Tris. Because Tris is able to occupy the substrate binding position, we speculate that this may be the basis for hKAT I inhibition. Furthermore, the hKAT/IAC complex structure reveals that the binding moieties of the inhibitor are its indole ring and a carboxyl group. Six chemicals with both binding moieties were tested for their ability to inhibit hKAT I activity; 3-indolepropionic acid and DL-indole-3-lactic acid demonstrated the highest level of inhibition, and as they cannot be considered as substrates of the enzyme, these two inhibitors are promising candidates for future study. Perhaps even more significantly, we report the discovery of two different ligands located simultaneously in the hKAT I active center for the first time.

Introduction

Human kynurenine aminotransferase I (hKAT[a] I) possesses broad amino acid specificity as an aminotransferase. The enzyme also catalyzes β-lyase reactions with several cysteine S-conjugates that contain a good leaving group in the β-position. The biologically significant product of this transamination reaction is kynurenic acid (KYNA). KYNA is the only known endogenous antagonist of *N*-methyl-D-aspartate subtype of glutamate receptors.[1−4] It also functions as an antagonist of the α7-nicotinic acetylcholine receptor.[5−8] KYNA was identified as an endogenous ligand for an orphan G-protein-coupled receptor (GPR35) that is predominantly expressed in immune cells.[9] Abnormal concentrations of KYNA have been observed in patients with multiple neurodegenerative diseases, including Huntington's disease,[10,11] Alzheimer's disease,[12] schizophrenia,[13−15] and acquired immunodeficiency syndrome dementia.[16] These data suggest that KYNA, acting as an endogenous modulator of glutamatergic and cholinergic neurotransmission, may be functionally significant. In addition to its role as an excitatory amino acid antagonist, KYNA is also involved in the control of the cardiovascular function by acting at the rostral ventrolateral medulla of the central nervous system.[17]

Spontaneously hypertensive rat, the most widely used animal model for studying genetic hypertension, is associated with abnormally low KYNA levels in the area of the central nervous system that fine-tunes physiological blood pressure.[18,19] The β-lyase reaction is thought to mediate the toxicity of the sulfur-containing fragments released from halogenated alkene derived cysteine S-conjugates.[20,21] Very recently, 5-*S*-L-cysteinyldopamine, the cysteine S-conjugate of dopamine, was identified as an aminotransferase substrate of hKAT I. This is particularly relevant to current biomedical research, as it is neurotoxic and may contribute to the nigral cell damage observed in Parkinson's disease.[22,23] Since KAT I activity is present in human brain, hKAT I may have a role in the pathogenesis or progression of Parkinson's disease. Because of its biochemical role in catalyzing these reactions, GTK/KAT I is of considerable interest to toxicologists and neurochemists.

hKAT I[24] is a fold type I aminotransferase,[25,26] characterized by the presence of an N-terminal arm, a small domain, and a large domain. A number of crystal structures of KAT enzymes[24,27−34] are available for further studies regarding putative inhibitors, substrates, or mechanisms of catalysis. Our previous study has shown that hKAT I activity was diminished around pH 7.5−8.0 when Tris was used as a buffer in hKAT I activity assays; indole-3-pyruvic acid and tryptophan also highly inhibited the hKAT I activity.[35] The detailed mechanism of these two compounds in hKAT I inhibition was not further explored. To understand the inhibition mechanism, we cocrystallized the proteins with Tris and indole-3-acetic acid (IAC, while structurally similar to indole-3-pyruvic acid, is not a substrate of hKAT I) and identified a possible inhibition mechanism through macromolecular crystallography.

Results

Overall Structure. The structures of hKAT I/inhibitor complexes were determined through molecular replacement and refined to 1.50 Å resolution for the hKAT I/Tris complex, 1.50 Å resolution for the hKAT I/glycerol (GOL) complex, and 1.55 Å resolution for the hKAT I/IAC complex. The final models contain 418 residues in each subunit and yield crystallographic R values of 18.0%, 17.5%, and 18.6% and R_{free} values of 20.0%, 19.5%, and 21.0% for the hKAT I/Tris, hKAT I/GOL, and the hKAT I/IAC complexes, respectively.

[||] The atomic coordinates and structure factors (codes 3fvs, sfvu, and 3fvx) have been deposited in the Protein Data Bank, Research Collaboratory for Structural Bioinformatics, Rutgers University, New Brunswick, NJ (http://www.rcsb.org).

* To whom correspondence should be addressed. Phone: 540-231-5779. Fax: 540-231-9070. E-mail: qianhan@vt.edu.
[†] Virginia Tech.
[‡] Brookhaven National Laboratory.
[#] NIDCR, National Institutes of Health.
[§] NINDS, National Institutes of Health.

[a] Abbreviations: GTK, glutamine transaminase K; GOL, glycerol; hKAT I, human kynurenine aminotransferase I; IAC, indole-3-acetic acid; KAT, kynurenine aminotransferase; KYNA, kynurenic acid; LLP, lysinepyridoxal 5′-phosphate; PLP, pyridoxal 5′-phosphate; PMP, pyridoxamine 5′-phosphate.

10.1021/jm9000874 CCC: $40.75
Published on Web 04/01/2009

Table 1. Data Collection and Refinement Statistics of hKAT I Crystals

	hKAT I/GOL	hKAT I/Tris	hKAT I/IAC
Crystal Data			
space group	*C*2	*C*2	*C*2
a (Å)	102.7	102.9	106.4
b (Å)	107.2	107.4	108.5
c (Å)	81.6	81.7	81.9
β (deg)	112.8	112.9	114.2
Data Collection			
X-ray source	BNL[a]-X29	BNL[a]-X29	BNL[a]-X29
wavelength (Å)	1.0809	1.0809	1.0809
resolution (Å)[b]	1.50 (1.55−1.50)	1.50 (1.55−1.50)	1.55 (1.61−1.55)
total no. of reflections	926 023	938 848	891 079
no. of unique reflections	129 484	129 473	122 095
R_{merge} [b]	0.06 (0.59)	0.08 (0.59)	0.05 (0.52)
I/s[b]	36.0 (3.1)	36.7 (3.8)	46.0 (3.8)
redundancy[b]	7.2 (6.7)	7.3 (6.9)	7.3 (6.9)
completeness (%)[b]	100.0 (100.0)	98.9 (97.6)	99.8 (100.0)
Refinement Statistics			
R_{work} (%)[b]	17.5 (24.6)	18.0 (22.0)	18.6 (26.6)
R_{free} (%)[b]	19.5 (27.6)	20.0 (24.9)	21.0 (30.8)
rms bond length (Å)	0.009	0.009	0.011
rms bond angle (deg)	1.275	1.285	1.330
no. of ligand or cofactor molecules[c]	2 LLP, 1 GOL	2 LLP, 1 Tris	2 LLP, 2 IAC, 5 GOL
no. of water molecules	702	664	590
average *B* overall (Å^2)	16.8	16.6	21.0
Ramachandran Plot Statistics (%)			
most favored	92.4	91.2	92.9
allowed	6.9	7.2	6.5
generously allowed	0.4	0.3	0.3
disallowed	0.3	0.3	0.3

[a] Brookhaven National Laboratory. [b] The values in parentheses are for the highest resolution shell. [c] LLP, lysinepyridoxal 5′-phosphate; GOL, glycerol; IAC, indo-3-acetic acid.

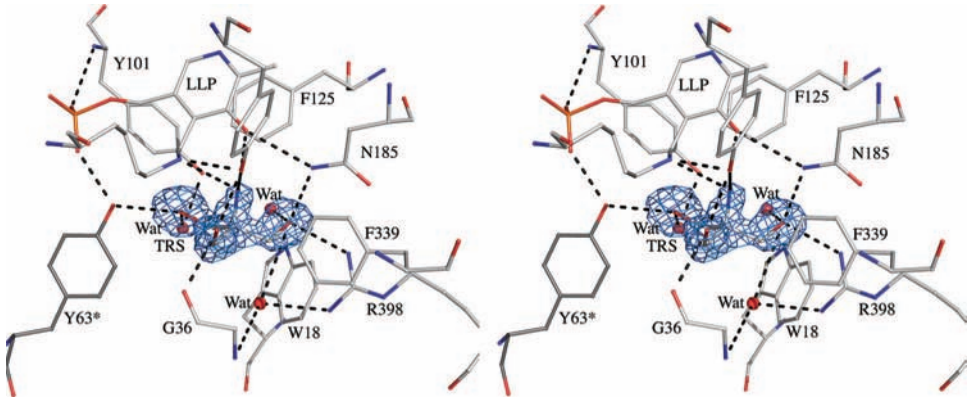

Figure 1. Tris binding site. The Tris molecule and the protein residues within 4 Å distance of Tris molecule are shown in stereo. The $2F_o - F_c$ electron density map covering Tris is shown contoured at the 0.9σ level.

All three complex structures have ideal geometry evaluated with PROCHECK[36] (Table 1). There are two protein molecules in an asymmetric unit that combine to form a biological homodimer. These residues of the two subunits in hKAT I complexes are numbered 4−422 for chain A and 4*−422* for chain B. The results of the refinement are summarized in Table 1. All residues except Phe278 are, in both chains, located in favorable regions of the Ramachandran plot as defined with PROCHECK.[36] However, Phe278 residues, in both complex structures, also fall within a favorable region of the Ramachandran plot when evaluated with Molprobity (URL, http://molprobity.biochem.duke.edu/). The first three residues (1−3) were not defined in the $2F_o - F_c$ and $F_o - F_c$ electron density maps and are absent from the final models. The protein architecture revealed by the hKAT I complex structures remains the same as the native hKAT I structure described previously.[24]

Electron density consistent with the presence of IAC was observed in the active sites of both subunits of the hKAT I/IAC complex (Figure 3, Figure S3 of Supporting Information), whereas only one of the monomers in the hKAT I/Tris complex showed electron density consistent with the presence of Tris (Figure 1, Figure S1 of Supporting Information).

Interactions of Tris and hKAT I. Inspection of the crystal structure of the hKAT I/Tris complex revealed that Tris lies near the PLP cofactor and that the Tris amine does not form an external aldimine with PLP. However, Tris is only seen in one of the two subunits of the biological dimer. In the active site of the subunit that does not contain a Tris molecule, there are three water molecules occupying the equivalent Tris position. This Tris molecule, three water molecules, and residues Gly36, Arg398, Tyr101, LLP, Asn185, Tyr216, Trp18, and Tyr63* form a hydrogen-bonding network in the enzyme active center. The

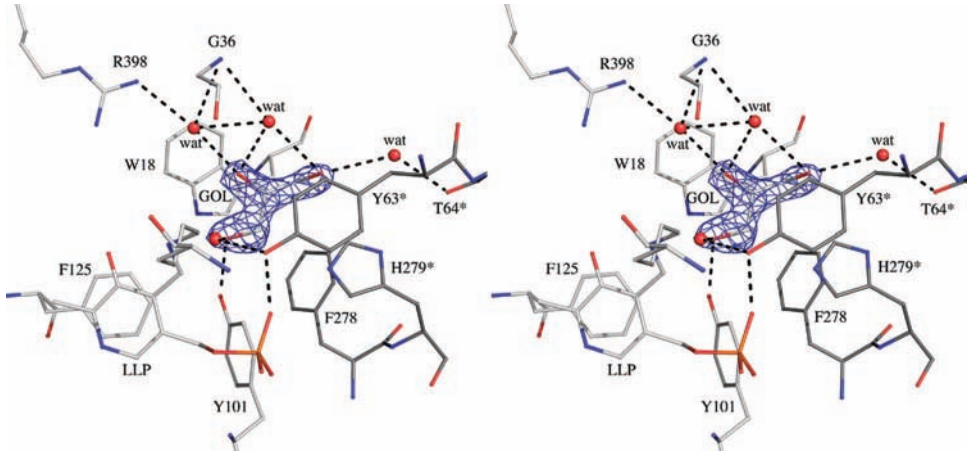

Figure 2. GOL binding site. GOL and the protein residues within 4 Å distance of GOL are shown in stereo. The residues in darker color, labeled with a star, are from the opposite chain. The $2F_o - F_c$ electron density map covering the GOL is shown contoured at the 1.8σ level.

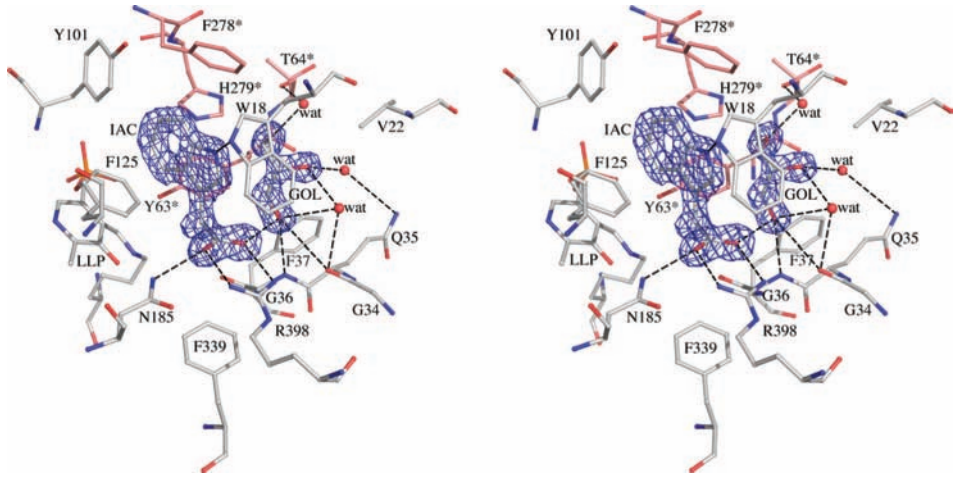

Figure 3. IAC and GOL interactions with hKAT I. IAC and GOL and the protein residues within 4 Å distance of both ligands are shown in stereo. The residues in pink color, labeled with a star, are from the opposite chain. The $2F_o - F_c$ electron density map covering the IAC and GOL is shown contoured at the 2.0σ level.

Tris molecule also contacts Phe125, Trp18, and Phe339 through hydrophobic interactions (Figure 1).

Interactions of Active Site Bound GOL and hKAT I. Like the interactions of Tris and hKAT I, GOL interacts with protein residues through a hydrogen-bonding network in the active center. GOL, four water molecules, and residues Gly36, Arg398, Tyr101, LLP, Tyr63*, Thr64* form this network. The other side of the GOL molecule also has hydrophobic interactions with residues Phe278, His279*, and Tyr63* (Figure 2, Figure S2 of Supporting Information). We tested the enzyme inhibition of GOL in the reaction mixture at concentrations ranging from 5% to 25%. GOL decreased the enzyme activity by about 10% only at a concentration of 25%. This seems to indicate that GOL is not a functional inhibitor of hKAT I. However, its extremely high concentration in the cryoprotection buffer may have facilitated its entry into the enzyme active center.

Interactions of IAC and hKAT I. As in the crystal structure of the hKAT I/Tris complex, the substrate lies near the PLP cofactor. However, the density map clearly shows that there is another compound occupying the active center. By carefully checking the $F_o - F_c$ and $2F_o - F_c$ maps, we identified the other compound in the center as GOL (Figure 4). The indole ring of IAC is inserted into a hydrophobic pocket formed by several residues, including LLP, Tyr63*, His279*, Phe278*, Tyr101, and Phe125. The carboxylic end of IAC forms a

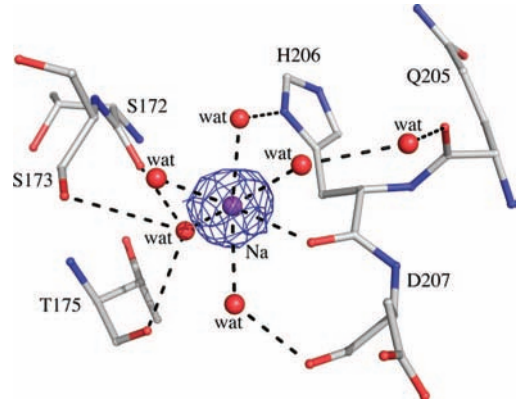

Figure 4. Na cation binding site. Na atom is shown in purple color, water O atoms are shown in red color, and the protein residues within 4 Å distance of Na atom are depicted as stick. The $2F_o - F_c$ electron density map covering the Na atom is shown contoured at the 1.8σ level.

hydrogen-bonding network, defined by Asn185, Gly36, Gly34, Arg398, Gln35, Thr64*, the GOL molecule, and three water molecules. IAC also forms a hydrogen bond with Trp18 in one subunit of the biological dimer. This is possible because one side of the GOL molecule has hydrophobic interactions with IAC and Phe37 and the other side of the molecule takes part in

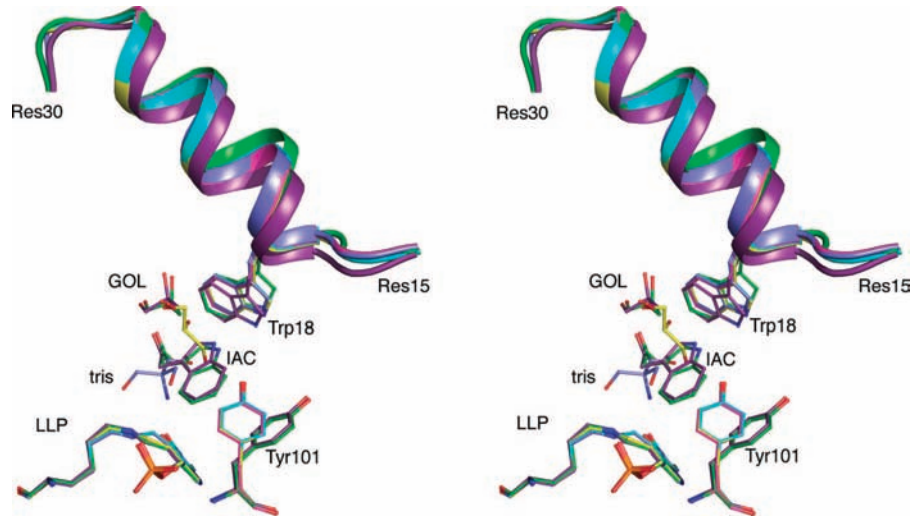

Figure 5. Superposition of two subunits of hKAT I/GOL structure (yellow and pink), two subunits of hKAT I/IAC complex structure (purple and green), and two subunits of hKAT I/Tris complex structure (blue and cyan). All the ligands and the residues with significant conformational change are shown in the figure. The protein residues 15−30 are shown in ribbon, and the other residues are depicted as stick.

the hydrogen-bonding network (Figure 3). Compared with the hKAT I/phenylalanine complex[24] previously reported, IAC has stronger hydrophobic interactions with the protein than phenylalanine. IAC also forms a hydrogen bond with Trp18, and phenylalanine does not.

Identification of Sodium Cation in hKAT I Structures. Since all three atomic complex structures were determined in high resolution, we carefully checked the water positions and found two water positions in each structure that are actually occupied by sodium cations. Sodium cations are located in the same positions in all six subunits of the three complex structures. This is not surprising, as the crystallization buffer contained at least 200 mM sodium acetate. The sodium atom is located in the center of an octahedron formed by five water molecules and the O atom of His206. The average bond length is 2.4 Å ranging from 2.2 to 2.7 Å between the Na and water O atoms (a total of 30 unique bond lengths) and also 2.4 Å ranging from 2.3 to 2.5 Å between the Na and O atoms of His206 (six unique bond lengths). The octahedron forms a hydrogen-bonding network with other residues, including Ser172, Ser173, Thr175, Asp207, and Gln205 (Figure 4, Figure S4 of Supporting Information). Sodium chloride (200 mM) did not affect hKAT I activity (result not shown), so the presence of sodium cations in the structure is not associated with enzyme activity. However, the Na atom is located directly between two small loops (structural turns), typically the flexible regions in protein structures. Furthermore, Lys176 located inside one of the turns forms a hydrogen bond with Leu5* from the N-terminal arm, and Val209 from the other turn has hydrophobic interaction with Leu5*, which may also decrease the flexibility of the N-terminal arm. By comparison of these three structures and the hKAT I structures previously published,[24] we do find that residues 4−6 at the N-terminal arm have high mobility. In fact, the phenylalanine-bound hKAT I crystal crystallized in sodium-salt-free medium only diffracted to 2.7 Å.[24] Therefore, the introduction of sodium cations into the structure most likely helps the crystallization of the protein, as each of these interactions work to decrease the flexibility of the N-terminal arm and two structural turns.

Comparison of Three Different Complex Structures. Through superposition of all six of the subunits from the three hKAT I structures, we observed a chain conformational change involving residues Asn16 to Asp29. The shift of the N-terminal α-helix (residues 17−27) toward the catalytic cavity changes the interaction between Trp18 and IAC by forming a hydrogen bond between them. The residue Tyr101 is displaced from the original position to make room for the incoming big ligand, IAC, but does not change conformation when the protein is bound by the smaller ligands, such as Tris or GOL (Figure 5).

Inhibition of hKAT I by Six Compounds with Both Indole Ring and Carboxyl Group. Six chemicals (3-indolepropionic acid, DL-indole-3-lactic acid, *trans*-3-indoleacrylic acid, indole-3-acetic acid, indole-3-pyruvic acid, and tryptophan) having both an indole ring and a carboxyl group were tested for the inhibition of hKAT I. Each chemical was incorporated into the reaction mixture (5 mM kynurenine, 5 mM α-ketobutyrate, and 2 μg of hKAT I in 50 μL in 100 mM phosphate buffer, pH 7.5) at final concentrations of 0.08, 0.16, 0.31, 0.63, 1.25, 2.50, 5.00, and 10.00 mM. These mixtures were incubated at 38 °C for 20 min, and the reaction was stopped by adding equal volumes of 1 M formic acid. The product KYNA was detected by high-performance liquid chromatography and quantified on the basis of the absorbance at 330 nm as measured by a Hitachi L-7400 UV detector. The assays for each inhibitor were performed four times, and the data were analyzed using the SigmaPlot enzyme kinetics module (SPSS Inc.). Figure 6A shows the chemical structures of the tested chemicals. Figure 6B shows the inhibitions of tryptophan and indole-3-pyruvic acid, and Figure 6C shows the inhibitions of the other four compounds. All six of the chemicals strongly inhibited hKAT I, and two of them were more effective in inhibiting the enzyme, i.e., 3-indolepropionic acid (IC_{50} = 0.14 ± 0.20 mM, mean ± SE, n = 4) and DL-indole-3-lactic acid (IC_{50} = 0.22 ± 0.22 mM, mean ± SE, n = 4). The kynurenine concentration used in the assay is based on the enzyme property.[35] Although the concentration is much higher than the physiological concentration (~2 μM),[37,38] it worked well in the enzyme inhibition tests or inhibitor screening. If the physiological concentration of kynurenine was tested, we would expect lower IC_{50} values because the inhibitors occupy the substrate binding sites and are competitive inhibitors.

Discussion

As we described in the Introduction, abnormally low concentrations of KYNA are associated with many neurodegenerative diseases. KYNA is known to have anticonvulsant and

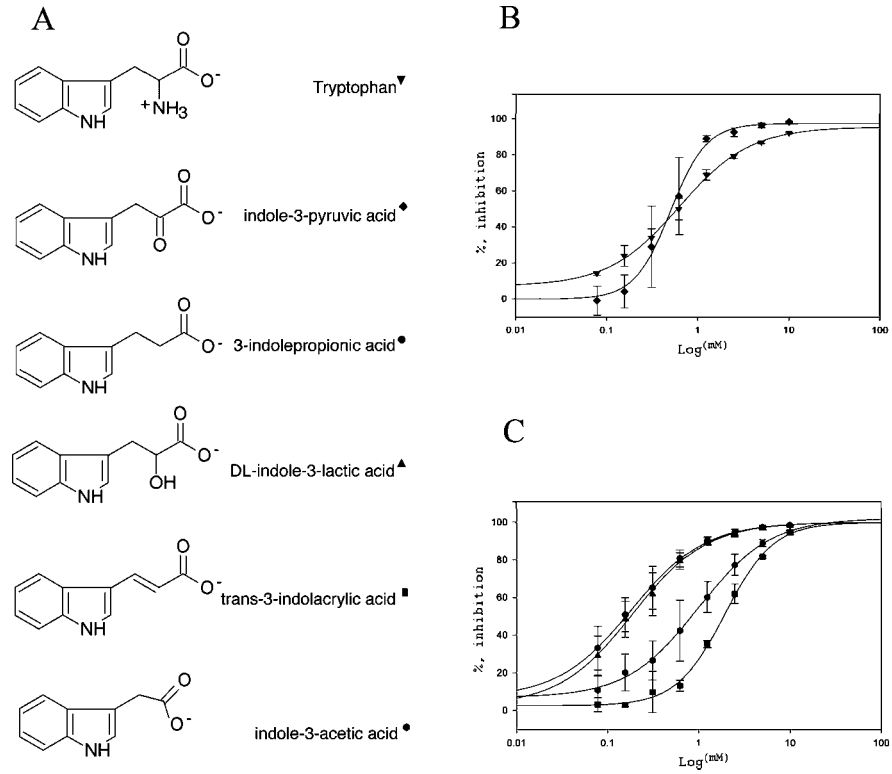

Figure 6. Chemical structures of six inhibitors and their inhibitions to hKAT I. The chemical structures of six tested compounds are shown in panel A. The inhibitions of tryptophan and indole-3-pyruvic acid are shown in panel B, and 3-indolepropionic acid, DL-indole-3-lactic acid, *trans*-3-indoleacrylic acid, and indole-3-acetic acid are shown in panel C.

neuroprotective effects,[39] and raising those concentrations may slow the progression of some forms of those diseases.[40,41] However, KYNA levels in the brain need to be well regulated, as high levels of KYNA can cause problems by diminishing the inhibition of the α7 nicotinic acetylcholine receptor function and enhancing glutamate release. Elevations of endogenous KYNA have also been implicated in spatial working memory deficits[42] and may contribute to the pathogenesis of schizophrenia.[15] The development of KAT inhibitors may prove useful in treating schizophrenia as well as disorders associated with learning and memory deficits, since lowering the levels of brain KYNA may counterbalance glutamatergic and cholinergic hypofunction.

Indole-3-pyruvic acid and tryptophan are the best inhibitors for hKAT I as reported in the previous study.[35] However, both compounds are also substrates of the enzyme and are present in the human body under physiological conditions. From the complex structure of hKAT I/IAC, we identified the major functional moieties facilitating binding as the indole ring and the carboxyl group in both competing inhibitors. On the basis of these results, we tested four more chemicals that are structurally similar to tryptophan or indole-3-pyruvic acid. All four of the chemicals have both the indole ring and carboxyl group moieties; the only differences are the links between the two binding groups. Owing to the lack of α-amino and α-keto groups, none of the four can be transaminated by hKAT I. Unlike competing substrates such as tryptophan, indole-3-pyruvic acid, cysteine, or glutamine,[35] these four chemicals can be expected to act as pure inhibitors. The tests that we have reported here indicate that 3-indolepropionic acid and DL-indole-3-lactic acid are the most effective inhibitors of the four. Therefore, they could be treated as promising candidates for future chemical modification studies identifying more effective inhibitors of hKAT I. Of particular interest is the fact that indole-3-pyruvic acid has been used in several clinical trials for promoting sleep and reducing anxiety[43] and could prove to be the first drug to enter into routine clinical use that was known a priori to act as a modulator of the kynurenine pathway.[41] The molecular mechanism of indole-3-pyruvic acid's function as an anxiolytic, however, is not clear. Nevertheless, it would be interesting to see if the inhibition of hKAT I plays a role in the anxiolytic function of indole-3-pyruvic acid in future studies.

We obtained crystals of three hKAT I complexes by cocrystallization with IAC, GOL, and Tris, respectively. The hKAT I/Tris complex structure shows Tris located in the enzyme active center and occupying the substrate binding site, indicating that at extremely high concentrations Tris may compete with substrates in the ligand binding. The kinetic and equilibrium studies of Tris and PLP showed that upon an increase of the pH from 7.3 to 9.3 at 25 °C, the apparent dissociation constant varies from 2 to 8 mM,[44] which explains why Tris and PLP bind less tightly when pH increases. In human mitochondrial branched-chain aminotransferase, Tris was found to bind the cofactor PLP and form a Schiff base in the protein structure.[45] Spectral shift of free PLP toward longer wavelengths in the presence of Tris at weak basic conditions was also observed in hKAT I, which suggests that Tris can interact with the enzyme-associated PLP.[46] In our complex structure we did not observe the Schiff base complex formation. However, Tris had already interacted with PLP through a hydrogen bond. If the pH was decreased in the buffer, Tris would compete with the Lys247 portion of the LLP enabling the formation of a Tris−PLP Schiff base. We previously found that the Tris inhibition of hKAT I is pH dependent, as significant inhibition is seen at pH 7.5 and 8 but not at pH 8.5.[46] We know that the pK_a value of Tris is 8.06 at 25 °C, so the Tris molecule is not charged at pH 8 or positively charged at pH 7.5. However, we do not know if the molecular charge affects the ability of Tris to enter into the

enzyme active center or if it affects the binding to hKAT I. Nonetheless, Tris at the active center of hKAT I could interfere with the substrate binding and internal aldimine formation and would therefore affect the enzyme activity.

hKAT I can use many different amino acids as amino group donors and various α-ketoacids as amino group acceptors in its transamination reaction. The substrates include such widely diverse compounds as hydrophilic glyoxylate, neutral amino acid glutamine, and aromatic amino acids with a hydrophobic (phenyl) or nearly hydrophobic (indolyl) group.[35] Even bigger molecules such as 5-*S*-L-cysteinyldopamine are acceptable substrates.[23] Unlike mosquito KAT, which has a large domain movement as a result of substrate binding,[27,30] hKAT I seems to bind substrates without a large domain movement except for the conformational change of the first N-terminal helix and Tyr101. The resulting conformational change is similar to mouse KAT III structures.[34] In hKAT I complex structures, including hKAT I/phenylalanine[24] and the three hKAT I structures reported here, the substrates/ligands reside at the active center; only large ligands change the side chain conformation of Tyr101. Tyr101 turns away from the original position to make room for the incoming substrate. Meanwhile the hydroxy group of Tyr101 shifts away from the wall of the binding cavity, forming a perfect hydrophobic pocket for an aromatic ligand, such as phenylalanine or IAC. Previously, it was proposed that substrate binding causes the shift of the N-terminal α-helix (residues Pro17-Glu27) toward the catalytic cavity, bringing the Trp18 into contact with the bound substrate.[24] However, we did not notice a significant conformational change in the N-terminal α-helix in complex with GOL or Tris; we only observed this type of conformational change (residues Asn16 to Asp29) in one of the ICA bound subunits (Figure 5). This observation indicates that only large ligands may cause this N-terminal α-helix shift. In *E. coli* aspartate aminotransferase, domain movement was changed dramatically from an open to a closed form by the addition of only one CH_2 to the side chain of the C4 substrate $CH_3(CH_2)C_\alpha H(NH_3)^+COO^-$.[47] Taken together, these results indicate that one of the two substrates (α-ketoacid and amino acid) must be big enough to initiate the conformational change in order for the transamination reaction to happen. Therefore, this could be used as a criterion for determining aminotransferase substrate specificity. In order to determine if an amino acid or α-ketoacid could act as the substrate of an aminotransferase, we need to consider the size of the substrate pair; at least one of them should be able to initiate a conformational change. However, we do not know how large a substrate would be needed to cause the required conformational change in hKAT I.

Unexpectedly, the N-terminal α-helix moved even further away from the catalytic center in one of the IAC bound subunits when compared with the unbound and Tris or GOL bound subunits (Figure 5). A careful check of the two subunits in the hKAT/IAC complex revealed that Trp18 has more contacts with subunit IAC in a closed shift of the N-terminal α-helix than in the open subunit with a shift of the N-terminal α-helix (Figure 5). This conformational change of the N-terminal α-helix might be mainly for plugging the active center and preventing the solvents from entering the catalytic cavity during the transamination reaction. Furthermore, the fact that the N-terminal α-helices from different subunits in the biological dimer of the hKAT I/IAC complex have different conformational changes is worthy of note. This could contribute one more piece of evidence indicating that the two subunits of aminotransferases may not be synchronized during the enzyme-catalyzed reaction through a ping-pong bi bi mechanism. Similar mechanisms were previously documented in the aromatic amino acid aminotransferase complex of the *Paracoccus denitrificans* with 3-phenylpropionate,[48] the alanine glyoxylate aminotransferase complex of *Aedes aegypti* with alanine,[49] and the KAT complex of mosquito with cysteine.[30]

By carefully checking the hKAT I complex structure with IAC, we observed two ligands in the active center: IAC and GOL. Among the crystal structures of KAT enzymes,[24,27−34] different intermediate structures have been reported, i.e., LLP form (internal aldimine), PMP form (with or without substrate binding), external aldimine, and Michaelis complexes with an amino acid substrate. In all previously reported structures of KAT enzymes, only one substrate was found at an active center of the complex structures. Here, for the first time, we report two ligands in the active center of hKAT I. This implies that the catalytic center has room to bind two ligands simultaneously. Since the size of IAC is similar to tryptophan, indole-3-pyruvic acid, or indole-3-glyoxylate and the size of GOL is approximately the same as glyoxylate or pyruvate, these two ligands could represent a pair of hKAT I substrates. Like all known aminotransferases, each of the hKAT I catalyzing centers conducts ping-pong bi bi reactions to catalyze the reaction from keto acid 1 and amino acid 2 to amino acid 1 and keto acid 2, respectively.[26] The ejection of the first product, for example, keto acid 2, from the enzyme active center requires the addition of the second substrate, amino acid 2. However, there is no evidence showing how the entry of a cosubstrate causes the ejection of the product from aminotransferases. The hKAT I complex that we describe here, with both IAC and GOL in the same active center, is perhaps a snapshot of this reaction. It may show the binding positions of the two substrates and that these two ligands interact with each other by hydrophobic interactions. If we put an α-ketoacid, glyoxylate, for example, in the position of GOL (Figure 3), we would see the carboxyl groups of glyoxylate and IAC form a hydrogen bond, which could be used in proton transfer during the reaction. This proton transfer could help the two ligands shift their positions resulting in the binding of the incoming substrate (amino acid 2) with Arg398, effectively replacing the product (keto acid 2) position.

Conclusions

A high-resolution hKAT I crystal structure complex with an inhibitor allowed us to identify more effective inhibitors of the enzyme. Among them, 3-indolepropionic acid and DL-indole-3-lactic acid could be considered lead inhibitors in future chemical modification studies. The complex in which two different substrate-like ligands are seen in one active center is described for the first time in KAT enzymes revealing the ephemeral linkages of hKAT I with these two ligands. This complex with two ligands in the active center provides a new intermediate structure for aminotransferase mechanisms and helps us better understand the overall process of transamination reactions. This paper also proposes possible mechanisms of Tris inhibition and the role of sodium cations in the crystallization of hKAT I.

Experimental Section

Chemicals. Six chemicals (3-indolepropionic acid (purity, 99%), DL-indole-3-lactic acid (99%), *trans*-3-indoleacrylic acid (99%), indole-3-acetic acid (≥99%), indole-3-pyruvic acid (98%), tryptophan (≥99%), and other chemicals used in the experiment were obtained from Sigma-Aldrich (St. Louis, MO).

Recombinant hKAT I. hKAT I was obtained according to the method used in our previous study[35] and stored at 4 °C at a

concentration of 10 mg/mL in 10 mM potassium phosphate buffer (pH 6.8). The specific activity assay for KAT was also performed according to a previous method.[35]

hKAT I Crystallization. The crystals were grown through hanging drop vapor diffusion methods with the volume of the reservoir solution at 500 μL and the drop volume at 2 μL, containing 1 μL of protein sample and 1 μL of reservoir solution. The crystallization buffer contained 22% PEG 4000, 0.2 M sodium acetate, 0.1 M Tris, pH 8.5. hKAT I/IAC complex was cocrystallized by adding 2.5 mM IAC and 4% glycerol (GOL) to the crystallization buffer, and hKAT I/GOL complex was cocrystallized by adding 5% GOL to the above crystallization buffer.

Data Collection and Processing. Individual hKAT I crystals were cryogenized in crystallization buffer containing 20% glycerol or 25% PEG 300 as a cryoprotectant. Diffraction data of hKAT I crystals were collected at the Brookhaven National Synchrotron Light Source beamline X29A ($\lambda = 1.0809$ Å). Data collection was done using an ADSC Q315 CCD detector. All data were indexed and integrated using HKL software.[50] Scaling and merging of diffraction data were performed using the program SCALEPACK.[51] The parameters of the crystals and information regarding data collection are described in Table 1.

Structure Determination. The structures of the hKAT I complexes were determined by the molecular replacement method using the published hKAT I structure without any ligands or water molecules (Protein Data Bank code 1W7L).[24] The program Molrep[52] in the CCP4 suite was employed to calculate both cross-rotation and translation function of the model. The initial model was subjected to iterative cycles of crystallographic refinement with Refmac 5.2[53] and graphic sessions for model building using the program O.[54] The substrate molecules were modeled when the *R* factor dropped to a value of 0.24 at full resolution for all hKAT I structures based on both the $2F_o - F_c$ and $F_o - F_c$ electron density maps. Solvent molecules were automatically added and refined by using ARP/wARP[55] together with Refmac 5.2.

Structure Analysis. Superposition of structures was done using Lsqkab[56] from the CCP4 suite. Figures were generated using Pymol.[57] Protein and substrate interactions were also analyzed using Pymol.[57]

Acknowledgment. This work was carried out in part at the National Synchrotron Light Source, Brookhaven National Laboratory, and supported in part by the Intramural Research Program of the institutes of NIDCR and NINDS at NIH. We are grateful to Elizabeth Watson and Graham Richardson (Dr. Jianyong Li's laboratory, Department of Biochemistry, Virginia Tech) for critical reading of this paper.

Supporting Information Available: Figures S1−S4 showing omit maps. This material is available free of charge via the Internet at http://pubs.acs.org.

References

(1) Leeson, P. D.; Iversen, L. L. The glycine site on the NMDA receptor: structure−activity relationships and therapeutic potential. *J. Med. Chem.* **1994**, *37* (24), 4053–4067.
(2) Perkins, M. N.; Stone, T. W. An iontophoretic investigation of the actions of convulsant kynurenines and their interaction with the endogenous excitant quinolinic acid. *Brain Res.* **1982**, *247* (1), 184–187.
(3) Stone, T. W.; Perkins, M. N. Actions of excitatory amino acids and kynurenic acid in the primate hippocampus: a preliminary study. *Neurosci. Lett.* **1984**, *52* (3), 335–340.
(4) Birch, P. J.; Grossman, C. J.; Hayes, A. G. Kynurenic acid antagonises responses to NMDA via an action at the strychnine-insensitive glycine receptor. *Eur. J. Pharmacol.* **1988**, *154* (1), 85–87.
(5) Pereira, E. F.; Hilmas, C.; Santos, M. D.; Alkondon, M.; Maelicke, A.; Albuquerque, E. X. Unconventional ligands and modulators of nicotinic receptors. *J. Neurobiol.* **2002**, *53* (4), 479–500.
(6) Hilmas, C.; Pereira, E. F.; Alkondon, M.; Rassoulpour, A.; Schwarcz, R.; Albuquerque, E. X. The brain metabolite kynurenic acid inhibits alpha7 nicotinic receptor activity and increases non-alpha7 nicotinic receptor expression: physiopathological implications. *J. Neurosci.* **2001**, *21* (19), 7463–7473.
(7) Alkondon, M.; Pereira, E. F.; Yu, P.; Arruda, E. Z.; Almeida, L. E.; Guidetti, P.; Fawcett, W. P.; Sapko, M. T.; Randall, W. R.; Schwarcz, R.; Tagle, D. A.; Albuquerque, E. X. Targeted deletion of the kynurenine aminotransferase ii gene reveals a critical role of endogenous kynurenic acid in the regulation of synaptic transmission via alpha7 nicotinic receptors in the hippocampus. *J. Neurosci.* **2004**, *24* (19), 4635–4648.
(8) Stone, T. W. Kynurenic acid blocks nicotinic synaptic transmission to hippocampal interneurons in young rats. *Eur. J. Neurosci.* **2007**, *25* (9), 2656–2665.
(9) Wang, J.; Simonavicius, N.; Wu, X.; Swaminath, G.; Reagan, J.; Tian, H.; Ling, L. Kynurenic acid as a ligand for orphan G protein-coupled receptor GPR35. *J. Biol. Chem.* **2006**, *281* (31), 22021–22028.
(10) Beal, M. F.; Matson, W. R.; Swartz, K. J.; Gamache, P. H.; Bird, E. D. Kynurenine pathway measurements in Huntington's disease striatum: evidence for reduced formation of kynurenic acid. *J. Neurochem.* **1990**, *55* (4), 1327–1339.
(11) Guidetti, P.; Reddy, P. H.; Tagle, D. A.; Schwarcz, R. Early kynurenergic impairment in Huntington's disease and in a transgenic animal model. *Neurosci. Lett.* **2000**, *283* (3), 233–235.
(12) Widner, B.; Leblhuber, F.; Walli, J.; Tilz, G. P.; Demel, U.; Fuchs, D. Tryptophan degradation and immune activation in Alzheimer's disease. *J. Neural Transm.* **2000**, *107* (3), 343–353.
(13) Schwarcz, R.; Rassoulpour, A.; Wu, H. Q.; Medoff, D.; Tamminga, C. A.; Roberts, R. C. Increased cortical kynurenate content in schizophrenia. *Biol. Psychiatry* **2001**, *50* (7), 521–530.
(14) Erhardt, S.; Blennow, K.; Nordin, C.; Skogh, E.; Lindstrom, L. H.; Engberg, G. Kynurenic acid levels are elevated in the cerebrospinal fluid of patients with schizophrenia. *Neurosci. Lett.* **2001**, *313* (1−2), 96–98.
(15) Erhardt, S.; Schwieler, L.; Nilsson, L.; Linderholm, K.; Engberg, G. The kynurenic acid hypothesis of schizophrenia. *Physiol. Behav.* **2007**, *92* (1−2), 203–209.
(16) Guillemin, G. J.; Kerr, S. J.; Brew, B. J. Involvement of quinolinic acid in AIDS dementia complex. *Neurotoxic. Res* **2005**, *7* (1−2), 103–123.
(17) Colombari, E.; Sato, M. A.; Cravo, S. L.; Bergamaschi, C. T.; Campos, R. R., Jr.; Lopes, O. U. Role of the medulla oblongata in hypertension. *Hypertension* **2001**, *38* (3, Part 2), 549–554.
(18) Ito, S.; Komatsu, K.; Tsukamoto, K.; Sved, A. F. Excitatory amino acids in the rostral ventrolateral medulla support blood pressure in spontaneously hypertensive rats. *Hypertension* **2000**, *35* (1, Part 2), 413–417.
(19) Kwok, J. B.; Kapoor, R.; Gotoda, T.; Iwamoto, Y.; Iizuka, Y.; Yamada, N.; Isaacs, K. E.; Kushwaha, V. V.; Church, W. B.; Schofield, P. R.; Kapoor, V. A missense mutation in kynurenine aminotransferase-1 in spontaneously hypertensive rats. *J. Biol. Chem.* **2002**, *277* (39), 35779–25782.
(20) McGoldrick, T. A.; Lock, E. A.; Rodilla, V.; Hawksworth, G. M. Renal cysteine conjugate C-S lyase mediated toxicity of halogenated alkenes in primary cultures of human and rat proximal tubular cells. *Arch. Toxicol.* **2003**, *77* (7), 365–370.
(21) Dekant, W.; Vamvakas, S.; Anders, M. W. Formation and fate of nephrotoxic and cytotoxic glutathione S-conjugates: cysteine conjugate beta-lyase pathway. *Adv. Pharmacol.* **1994**, *27*, 115–162.
(22) Spencer, J. P.; Whiteman, M.; Jenner, P.; Halliwell, B. 5-*s*-Cysteinyl-conjugates of catecholamines induce cell damage, extensive DNA base modification and increases in caspase-3 activity in neurons. *J. Neurochem.* **2002**, *81* (1), 122–129.
(23) Cooper, A. J.; Pinto, J. T.; Krasnikov, B. F.; Niatsetskaya, Z. V.; Han, Q.; Li, J.; Vauzour, D.; Spencer, J. P. Substrate specificity of human glutamine transaminase K as an aminotransferase and as a cysteine S-conjugate beta-lyase. *Arch. Biochem. Biophys.* **2008**, *474* (1), 72–81.
(24) Rossi, F.; Han, Q.; Li, J.; Li, J.; Rizzi, M. Crystal structure of human kynurenine aminotransferase I. *J. Biol. Chem.* **2004**, *279* (48), 50214–50220.
(25) Jansonius, J. N. Structure, evolution and action of vitamin B6-dependent enzymes. *Curr. Opin. Struct. Biol.* **1998**, *8* (6), 759–769.
(26) Eliot, A. C.; Kirsch, J. F. Pyridoxal phosphate enzymes: mechanistic, structural, and evolutionary considerations. *Annu. Rev. Biochem.* **2004**, *73*, 383–415.
(27) Han, Q.; Gao, Y. G.; Robinson, H.; Ding, H.; Wilson, S.; Li, J. Crystal structures of *Aedes aegypti* kynurenine aminotransferase. *FEBS J.* **2005**, *272* (9), 2198–2206.
(28) Goto, M.; Omi, R.; Miyahara, I.; Hosono, A.; Mizuguchi, H.; Hayashi, H.; Kagamiyama, H.; Hirotsu, K. Crystal structures of glutamine: phenylpyruvate aminotransferase from *Thermus thermophilus* HB8: induced fit and substrate recognition. *J. Biol. Chem.* **2004**, *279* (16), 16518–16525.
(29) Wogulis, M.; Chew, E. R.; Donohoue, P. D.; Wilson, D. K. Identification of formyl kynurenine formamidase and kynurenine aminotransferase from *Saccharomyces cerevisiae* using crystallo-

graphic, bioinformatic and biochemical evidence. *Biochemistry* **2008**, *47* (6), 1608–1621.
(30) Han, Q.; Gao, Y. G.; Robinson, H.; Li, J. Structural insight into the mechanism of substrate specificity of Aedes kynurenine aminotransferase. *Biochemistry* **2008**, *47* (6), 1622–1630.
(31) Rossi, F.; Garavaglia, S.; Montalbano, V.; Walsh, M. A.; Rizzi, M. Crystal structure of human kynurenine aminotransferase II, a drug target for the treatment of schizophrenia. *J. Biol. Chem.* **2008**, *283* (6), 3559–3566.
(32) Han, Q.; Robinson, H.; Li, J. Crystal structure of human kynurenine aminotransferase II. *J. Biol. Chem.* **2008**, *283* (6), 3567–3573.
(33) Han, Q.; Cai, T.; Tagle, D. A.; Robinson, H.; Li, J. Substrate specificity and structure of human aminoadipate aminotransferase/kynurenine aminotransferase II. *Biosci. Rep.* **2008**, *28* (4), 205–215.
(34) Han, Q.; Robinson, H.; Cai, T.; Tagle, D. A.; Li, J. Biochemical and structural properties of mouse KAT III. *Mol. Cell. Biol.* **2009**, *29* (3), 784–793.
(35) Han, Q.; Li, J.; Li, J. pH dependence, substrate specificity and inhibition of human kynurenine aminotransferase I. *Eur. J. Biochem.* **2004**, *271*, 4804–4814.
(36) Laskowski, R. A.; Macarthur, M. W.; Moss, D. S.; Thornton, J. M. Procheck, a program to check the stereochemical quality of protein structures. *J. Appl. Crystallogr.* **1993**, *26*, 283–291.
(37) Chiarugi, A.; Carpenedo, R.; Moroni, F. Kynurenine disposition in blood and brain of mice: effects of selective inhibitors of kynurenine hydroxylase and of kynureninase. *J. Neurochem.* **1996**, *67* (2), 692–698.
(38) Ceresoli-Borroni, G.; Schwarcz, R. Perinatal kynurenine pathway metabolism in the normal and asphyctic rat brain. *Amino Acids* **2000**, *19* (1), 311–323.
(39) Wu, H. Q.; Lee, S. C.; Scharfman, H. E.; Schwarcz, R. L-4-Chlorokynurenine attenuates kainate-induced seizures and lesions in the rat. *Exp. Neurol.* **2002**, *177* (1), 222–232.
(40) Schwarcz, R. The kynurenine pathway of tryptophan degradation as a drug target. *Curr. Opin. Pharmacol.* **2004**, *4* (1), 12–17.
(41) Stone, T. W.; Darlington, L. G. Endogenous kynurenines as targets for drug discovery and development. *Nat. Rev. Drug Discovery* **2002**, *1* (8), 609–620.
(42) Chess, A. C.; Simoni, M. K.; Alling, T. E.; Bucci, D. J. Elevations of endogenous kynurenic acid produce spatial working memory deficits. *Schizophr. Bull.* **2007**, *33* (3), 797–804.
(43) Politi, V.; De Luca, G.; Gallai, V.; Puca; Comin, M. Clinical experiences with the use of indole-3-pyruvic acid. *Adv. Exp. Med. Biol.* **1999**, *467*, 227–232.
(44) Davis, M. D.; Edmondson, D. E.; McCormick, D. B. Reaction of pyridoxal 5′-phosphate with tris. *Monatsh. Chem.* **1982**, *113*, 999–1005.
(45) Yennawar, N.; Dunbar, J.; Conway, M.; Hutson, S.; Farber, G. The structure of human mitochondrial branched-chain aminotransferase. *Acta Crystallogr., Sect. D: Biol. Crystallogr.* **2001**, *57* (Part 4), 506–615.
(46) Han, Q.; Li, J. Cysteine and keto acids modulate mosquito kynurenine aminotransferase catalyzed kynurenic acid production. *FEBS Lett.* **2004**, *577* (3), 381–385.
(47) Ishijima, J.; Nakai, T.; Kawaguchi, S.; Hirotsu, K.; Kuramitsu, S. Free energy requirement for domain movement of an enzyme. *J. Biol. Chem.* **2000**, *275* (25), 18939–18945.
(48) Okamoto, A.; Nakai, Y.; Hayashi, H.; Hirotsu, K.; Kagamiyama, H. Crystal structures of *Paracoccus denitrificans* aromatic amino acid aminotransferase: a substrate recognition site constructed by rearrangement of hydrogen bond network. *J. Mol. Biol.* **1998**, *280* (3), 443–461.
(49) Han, Q.; Robinson, H.; Gao, Y. G.; Vogelaar, N.; Wilson, S. R.; Rizzi, M.; Li, J. Crystal structures of *Aedes aegypti* alanine glyoxylate aminotransferase. *J. Biol. Chem.* **2006**, *281* (48), 37175–37182.
(50) Otwinowski, Z. *Data Collection and Processing*; Daresbury Laboratory: Warrington, U.K., 1993; pp 56−62.
(51) Minor, W. *XDISPLAYF Program*; Purdue University: West Lafayette, IN, 1993.
(52) Vagin, A.; Teplyakov, A. MOLREP: an automated program for molecular replacement. *J. Appl. Crystallogr.* **1997**, *30*, 1022–1025.
(53) Murshudov, G. N.; Vagin, A. A.; Dodson, E. J. Refinement of macromolecular structures by the maximum-likelihood method. *Acta Crystallogr., Sect. D: Biol. Crystallogr.* **1997**, *53* (Part 3), 240–255.
(54) Jones, T. A.; Zou, J. Y.; Cowan, S. W.; Kjeldgaard, M. Improved methods for building protein models in electron density maps and the location of errors in these models. *Acta Crystallogr. A* **1991**, *47* (Part 2), 110–119.
(55) Perrakis, A.; Sixma, T. K.; Wilson, K. S.; Lamzin, V. S. wARP: improvement and extension of crystallographic phases by weighted averaging of multiple refined dummy atomic models. *Acta Crystallogr. D* **1997**, *53*, 448–455.
(56) Kabsch, W. Crystal physics, diffraction, theoretical and general crystallography. *Acta Crystallogr.* **1976**, *A32*, 922–923.
(57) DeLano, W. L. *The PyMOL Molecular Graphics System*; Delano Scientifc: San Carlos, CA, 2002.

JM9000874